Underwater Noise in Offshore Impact Piling Including Pile-Soil Contact Relaxation

Canny, Khairina A.; Peng, Yaxi; Tsetas, Athanasios; Tsouvalas, Apostolos

Publication date
2025

Document Version
Final published version

Published in
UACE 2025 Conference Proceedings

Underwater Noise in Offshore Impact Piling Including Pile-Soil Contact Relaxation

Canny, Khairina A.[1], Peng, Yaxi[1], Tsetas, Athanasios[1], and Tsouvalas, Apostolos[1]

[1]Department of Civil Engineering and Geosciences, Delft University of Technology

Corresponding author's email:

Abstract: *As the trend shifts toward the installation of larger foundation piles for offshore wind farms, which are associated with lower frequency excitations, accurately predicting the resulting sound and vibrations requires a precise characterization of soil behaviour and pile-soil interaction. In addition to noise emissions caused by pile installation, substrate-borne vibrations are particularly perceptible to various marine biota. Both seabed vibrations and underwater noise raise concerns about ecological impacts, emphasizing the need for predictive models that accurately represent the interactions between pile, soil, and seawater. This paper examines the effects of the inclusion of the pile-soil contact mechanism during impact pile driving both in the underwater soundand the seabed vibrations. The pile-soil mechanism condition is modelled by the introduction of linear springs at thepile-soil interface allowing for relative displacement to develop between the soil and the pile. A case study is conducted to explore the implications of the contact mechanism, focusing on the two key outputs: the noise levels in thesurrounding fluid and particle motion within the substrate. Sensitivity analysis is performed to evaluate how variations in contact conditions during impact piling influence these critical metrics.*

Keywords: *underwater noise, offshore pile driving, fluid-soil-structure interaction, contact stress relaxation*

1. INTRODUCTION

Offshore wind energy is scaling rapidly, with turbine sizes increasing and foundation systems requiring larger and deeper-installed piles. These large-diameter monopiles introduce complex dynamic behavior, particularly in the low-frequency range, where soil-pile interaction becomes a dominant factor in the response. Growing evidence confirms that low-frequency substrate vibrations affect fish and aquatic invertebrates, as shown in recent studies [1, 2]. To better predict these environmental impacts, a more realistic fluid-soil-pile interaction model should account for the contact mechanism. Seminal works by Tsouvalas and Metrikine [3] and Peng et

al. [4] used semi-analytical vibroacoustic models to account for elastic properties of the marine sediment, emphasizing the role of interface waves. Tsetas et al. [5] extended this approach to vibratory pile driving, introducing non-linear contact mechanisms between pile and soil (i.e. history dependent friction). Building on this, Molenkamp et al. [6] employed a two-step boundary element approach to couple pile dynamics with acoustic propagation, finding that contact mechanism reduces Scholte wave amplitudes but enhances near-resonant pile motion. Bohne et al. [7] explored these dynamics numerically for smaller impact-driven piles, while Di et al. [8] addressed soil-pile behaviour in the interface in the context of nondestructive testing. This paper extends the semi-analytical model of [3] by explicitly incorporating pile-soil contact mechanism into impact pile driving scenarios. This sections are organized as follows. The next section introduces the fundamental geometrical configuration and material properties of the model. In Section 2, we derive the governing equations for the cylindrically symmetric case, providing the analytical foundation of the proposed method. Section 3 presents a case study to analyze the effects of soil contact stress relaxation. Finally, Section 4 summarizes the main findings and discusses potential directions for future research.

2. CYLINDRICALLY SYMMETRIC CASE

In this section, we derive the complete set of governing equations for the cylindrically symmetric configuration, following the framework established in [3, 4]. Our formulation extends previous models by incorporating a contact mechanism at the pile-soil interface, modeled through a viscoelastic constitutive relation.

2.1. MODEL DESCRIPTION AND GOVERNING EQUATIONS

The near-source model of impact pile driving is illustrated in Figure 1. In this model, the pile is represented as a shell occupying the domain $0 \leq z \leq L$. Surrounding the pile, the fluid domain is modeled as a three-dimensional, inviscid, and compressible medium, characterized by a compressional wave speed c_f and mass density ρ_f. The fluid occupies the region $z_0 \leq z \leq z_1$, where z_0 and z_1 correspond to the sea surface and seabed levels, respectively. Below the seabed, the soil is described as a three-dimensional elastic medium with density ρ_s, and compressional and shear wave velocities c_p and c_s, respectively. In the near-source approach, the soil extends downward from the seabed ($z = z_1$) to the bedrock level ($z = z_2$). The soil-pile interaction is bounded at a lower depth $z = L$ by a rigid boundary, which has been shown to exert a negligible influence on the dynamic response of the pile and, by extension, on the mechanisms of underwater noise generation. The governing equations for this coupled system are derived in line with the formulation presented in [4], and are expressed in Equations (1)–(2), which describe the dynamic behavior of the pile, fluid, and soil domains under impact loading conditions.

$$\mathbf{L}\mathbf{u}_{pl} + \mathbf{I}_m \ddot{\mathbf{u}}_{pl} = -[H(z - z_1) - H(z - L)]\mathbf{t}_s + [H(z - z_0) - H(z - z_1)]\mathbf{p}_f + \mathbf{f} \quad (1)$$

$$\nabla^2 p_f(r, z, t) - \frac{1}{c_f^2}\ddot{p}_f(r, z, t) = 0 \quad \text{and} \quad (\lambda + 2\mu)\nabla(\nabla \cdot \mathbf{u}_s) - \mu\nabla \times (\nabla \times \mathbf{u}_s) = \rho_s \ddot{\mathbf{u}}_s \quad (2)$$

The notation $\mathbf{L}$ and $\mathbf{I}_m$ represent the stiffness and inertial matrices, respectively following the formulation provided in [5]. The pile displacement vector is denoted by $\mathbf{u}_{pl}(z, t) =$

$[u_{pl,r}, u_{pl,z}]^{\mathrm{T}}$, where $u_{pl,r}$ and $u_{pl,z}$ correspond to the radial and vertical displacements in the axisymmetric case. These components describe the dynamic deformation of the pile under external and internal forces. The external force acting on the pile surface is represented as $\mathbf{f}(z,t) = [f_{rr}, f_{rz}]^{\mathrm{T}}$, accounting for the radial and shear tractions imposed by the surrounding medium. The function $H(z - z_i)$ denotes the Heaviside step function, which is used to activate the material interfaces at specific depths within the fluid and soil domains.

The governing equations that characterize the dynamic response of the fluid and the elastic soil media are described in Equation (2). A Helmholtz decomposition is employed to facilitate their analytical solution. Specifically, the velocity field in the fluid is represented as $\mathbf{v}_f = \nabla\phi_f$. The displacement field in the elastic soil medium is expressed as $\mathbf{u}_s = \nabla\phi_s + \nabla \times \left(0, -\frac{\partial \psi_s}{\partial r}, 0\right)$. These scalar and vector potentials represent compressional and shear wave components, respectively, and allow to decouple the elastic wave propagation modes. Applying the Fourier transform, the elastic wave equation can be written in terms of the potential functions, capturing both compressional and shear behavior in the soil medium. These potentials are written as (3)

$$\begin{aligned} \nabla^2\tilde{\phi}_f(r,z,\omega) &= -\frac{\omega^2}{c_f^2}\tilde{\phi}_f(r,z,\omega) \\ \nabla^2\tilde{\phi}_s(r,z,\omega) &= -\frac{\omega^2}{c_p^2}\tilde{\phi}_s(r,z,\omega); \quad \nabla^2\tilde{\psi}_s(r,z,\omega) = -\frac{\omega^2}{c_s^2}\tilde{\psi}_s(r,z,\omega) \end{aligned} \tag{3}$$

The notations ϕ_f, ϕ_s, and ψ_s denotes the fluid potential, soil compressional potential, and soil shear potential, respectively.

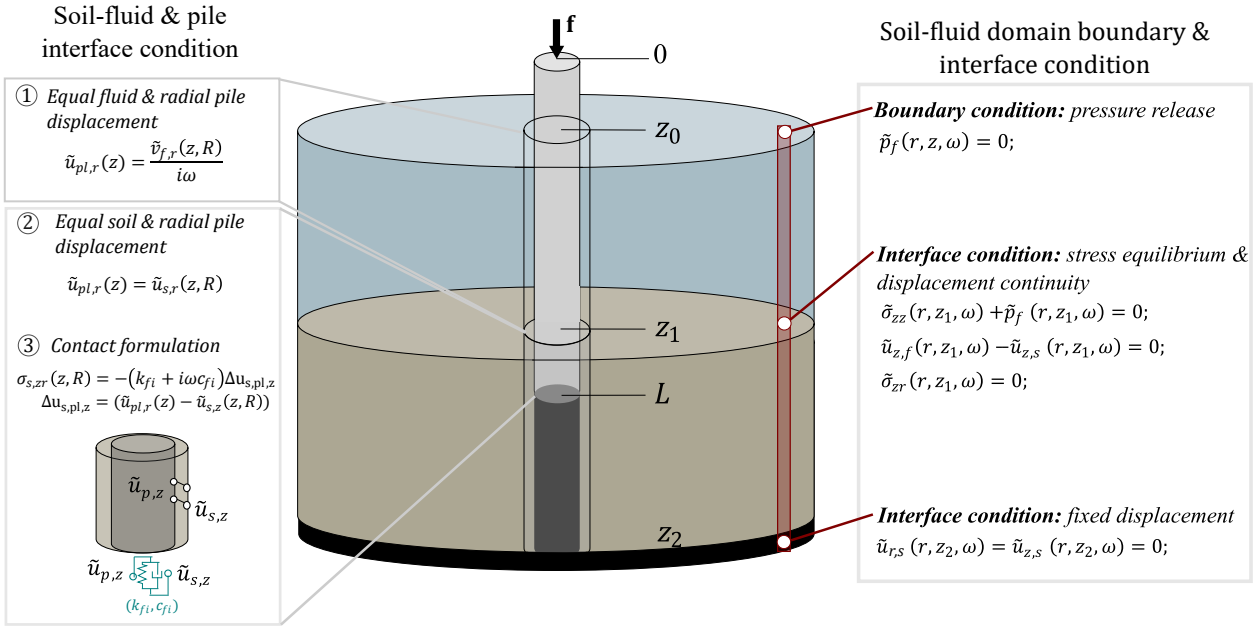

Figure 1: Illustration of the model description for fluid-soil-pile interaction and the contact interface representation using elastic spring-dashpot.

2.2. SOLUTION TO THE COUPLED VIBROACOUSTIC PROBLEM

The modal matching technique employed in the near field model builds upon the framework established in the study by Tsouvalas [3] and Peng [4], and the modal representation used to model the shell structure uses the approach developed in [5]. Applying the work of Tsetas et al. [5], the semi-analytical finite element (SAFE) model is applied for thin shells, which is based on the Love-Timoshenko shell theory; consequently, the shell displacement incorporating both radial and axial motion is expressed as a modal summation in Equations (4), where each mode satisfies the governing equations and boundary conditions of the shell structure.

$$\tilde{u}_{pl,r}(z,\omega) = \sum_{m=1}^{\infty} A_{0m} U_{pl,r0m}(z) \quad \text{and} \quad \tilde{u}_{pl,z}(z,\omega) = \sum_{m=1}^{\infty} A_{0m} U_{pl,z0m}(z) \tag{4}$$

The unknown modal constants, A_{0m}, will be determined through the coupled system, with the subscript m denoting the axial mode number. In this context, the terms $U_{pl,r0m}$ and $U_{pl,z0m}$ represent the pile eigenvectors in the radial and vertical directions, respectively.

As for the fluid potentials, the solution satisfying the interface and boundary conditions shown in Figure 1 is expressed as a summation of modes, as given by Equations (5):

$$\begin{aligned} \tilde{v}_{f,z}(r,z,\omega) &= \sum_{p=1}^{\infty} C_p H_0^{(2)}(k_p r)\tilde{v}_{f,z,p}(z); \quad \tilde{v}_{f,r}(r,z,\omega) = \sum_{p=1}^{\infty} C_p H_1^{(2)}(k_p r)\tilde{v}_{f,r,p}(z) \\ \tilde{p}_f(r,z,\omega) &= \sum_{p=1}^{\infty} C_p H_0^{(2)}(k_p r)\tilde{p}_{f,p}(z) \end{aligned} \tag{5}$$

Likewise, the soil potentials satisfy the interface and boundary conditions, as shown in Figure 1). Therefore, they are expressed as a summation of modes, as written in Equation (6)

$$\begin{aligned} \tilde{u}_{s,z}(r,z,\omega) &= \sum_{p=1}^{\infty} C_p H_0^{(2)}(k_p r)\tilde{u}_{s,z,p}(z); \quad \tilde{u}_{s,r}(r,z,\omega) = \sum_{p=1}^{\infty} C_p H_0^{(2)}(k_p r)\tilde{u}_{s,r,p}(z) \\ \tilde{\sigma}_{s,zz}(r,z,\omega) &= \sum_{p=1}^{\infty} C_p H_0^{(2)}(k_p r)\sigma_{s,zz,p}(z); \quad \tilde{\sigma}_{s,zr}(r,z,\omega) = \sum_{p=1}^{\infty} C_p H_1^{(2)}(k_p r)\sigma_{s,zr,p}(z) \\ \tilde{\sigma}_{s,rr}(r,z,\omega) &= \sum_{p=1}^{\infty} C_p \left(H_0^{(2)}\tilde{\sigma}_{s,rr,p}^{H_0}(z) + \frac{1}{r} H_1^{(2)}\tilde{\sigma}_{s,rr,p}^{H_1}(z) \right) \end{aligned} \tag{6}$$

The soil displacement in the radial and vertical directions is represented as $\tilde{u}_{s,r}$ and $\tilde{u}_{s,z}$, respectively. The stresses in the soil, expressed in cylindrical coordinates, are denoted by $\sigma_{s,zr}$, $\sigma_{s,rr}$, and $\sigma_{s,zz}$. Additionally, C_p is a complex-valued coefficient determined by solving the force response of the coupled system. The functions $H_0^{(2)}$ and $H_1^{(2)}$ are the Hankel functions of the second kind, which describe the propagation of cylindrical waves in an unbounded medium.

Interface condition 1: The radial velocity at the fluid level must match the radial velocity at the pile interface. This is expressed as $i\omega \cdot \tilde{u}_{pl,r}(z,\omega) = \tilde{v}_{f,r}(R,z,\omega)$ within the fluid domain $z_0 < z < z_1$ and at the pile interface $r = R$. The detailed expression for this condition is substituted from Equations (5) and (6). This interface condition is represented as Equation (7):

$$i\omega \sum_{m=1}^{\infty} A_{0m} \cdot U_{pl,r,0m}(z) = \sum_{p=1}^{\infty} C_p \cdot H_1^{(2)}(k_p R)\tilde{v}_{f,r,p}(z) \tag{7}$$

Interface condition 2: The displacement in the radial direction is continuous across the pile and soil interface. This condition is written as $\tilde{u}_{pl,r}(z,\omega) = \tilde{u}_{s,r}(R,z,\omega)$ within the soil domain $z_1 < z < L$ and at the pile interface $r = R$. The expression for this condition is substituted from Equations (5) and (6). The corresponding interface condition is given by Equation (8):

$$\sum_{m=1}^{\infty} A_{0m} \cdot U_{pl,r,0m}(z) = \sum_{p=1}^{\infty} C_p \cdot H_1^{(2)}(k_p R)\tilde{u}_{s,r,p}(z) \tag{8}$$

Interface condition 3: A constitutive relation for the contact in the z-direction is introduced, incorporating an elastic spring and dashpot at the pile contact interface, denoted as k_{fi} and c_{fi}, respectively, as shown in Figure 1. This relation is expressed as $\tilde{\sigma}_{s,zr}(z,r,\omega) = -(k_{fi}+i\omega c_{fi})\cdot \big(\tilde{u}_z(z) - \tilde{u}_{s,z}(z)\big)$ within the soil domain $z_1 < z < L$ and at the pile interface $r = R$. The corresponding form, derived from Equations (5) and (6), is given in Equation (9):

$$\tilde{\sigma}_{s,zr}(z,r,\omega) = -(k_{fi} + i\omega c_{fi}) \left(\sum_{m=1}^{\infty} A_{0m} \cdot U_{pl,z,0m}(z) - \sum_{p=1}^{\infty} C_p \cdot H_0^{(2)}(k_p R)\tilde{u}_{s,z,p}(z) \right) \tag{9}$$

In order to ensure the stability of Equation (9), we divide both sides of the Equation by $(k_{fi} + i\omega c_{fi})$. This results in the following equation (10):

$$-\frac{\sum_{p=1}^{\infty} C_p H_1^{(2)}(k_p r)\sigma_{s,zr,p}(z)}{(k_{fi} + i\omega c_{fi})} + \sum_{p=1}^{\infty} C_p \cdot H_0^{(2)}(k_p R)\tilde{u}_{s,z,p}(z) = \sum_{m=1}^{\infty} A_{0m} \cdot U_{z,0m}(z) \tag{10}$$

Meanwhile, the full contact limit ($\lim_{k_{fi}\to\infty}$) effectively cancels out the first term in equation (10), resulting in $\sum_{m=1}^{\infty} A_{0m}\, U_{z,0m}(z) = \sum_{p=1}^{\infty} C_p\, H_0^{(2)}(k_p R)\, \tilde{u}_{s,z,p}(z)$. To proceed, the operations on Equations (7), (8), and (10) are carried out to obtain the soil-fluid orthogonality. Afterwards, the modal matching method is applied to solve the pile-soil-fluid interaction. These steps follow the same framework as outlined in reference [3]. However, the main modification in the subsequent analysis will be in Equation (10), where the introduction of the spring-dashpot contact model alters the interaction terms between the soil and pile.

3. CASE STUDY

In this section, we examine the impact of contact mechanism on the interaction between the pile and the surrounding soil. Through a sensitivity analysis, we explore how changes in the contact parameters influence the system, with a particular focus on large pile diameters. The case study, as depicted in Figure 2, highlights the key features and setup for this analysis.

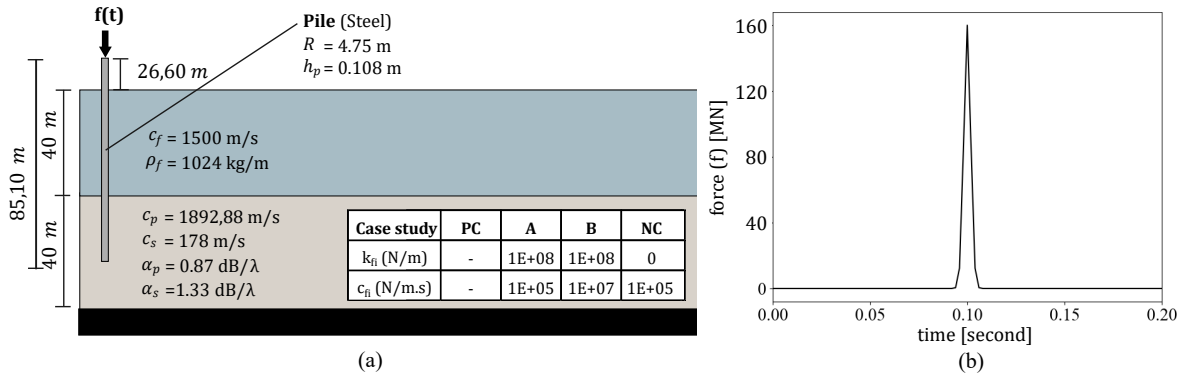

Figure 2: The case study properties: (a) the basic dimension and the sensitivity analysis for multiple contact parameters; (b) the hammer force in time domain.

The overall fluid pressure in the time domain, as shown in Figure 3, along with the snapshots of the pressure field in Figure 4, both reveal that the fluid pressure oscilation increase as the contact at the pile-soil interface is relaxed.

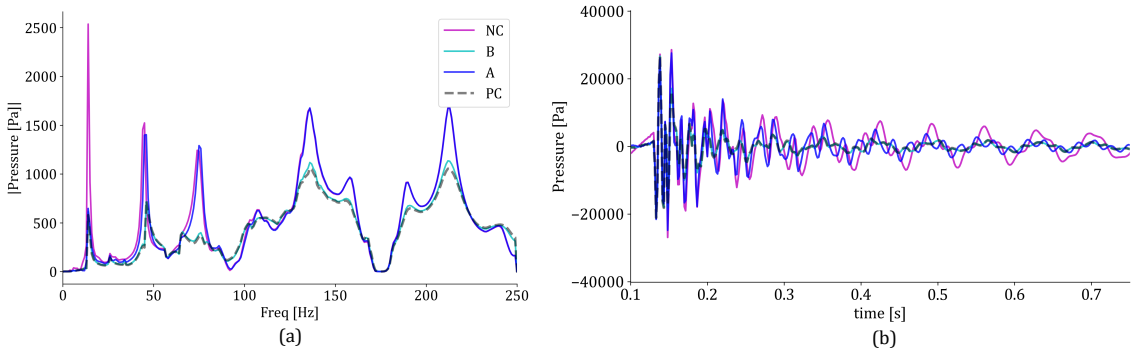

Figure 3: The fluid pressure at r =40m and z=20m: (a) Frequency response of the fluid pressure under 1MN constant amplitude frequency sweep and (b) time-domain fluid pressure.

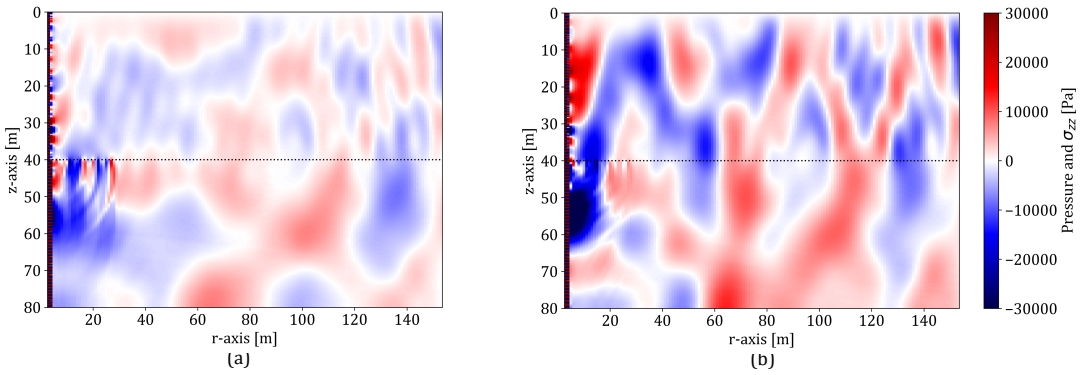

Figure 4: The fluid pressure and soil stress field snapshot at t=0.25 second: (a) perfect contact (PC), and (b) no contact (NC).

In contrast to the fluid pressure, Figures 5 and 6 illustrate that seabed soil vibrations decrease as the contact condition is relaxed compared to the perfect contact case. This holds true for

both the radial and vertical directions. These trends align with the frequency-domain analysis presented in Figures 5a and 6a. Moreover, increasing the damping constant (Case B) leads to a reduction in the pile dynamics, which, in turn, results in a decrease in fluid pressure oscillation and an increase in soil vibration, as seen in Figure 3,5, and 6. As the contact damping increases, the system's response gradually approaches the one observed under perfect contact conditions.

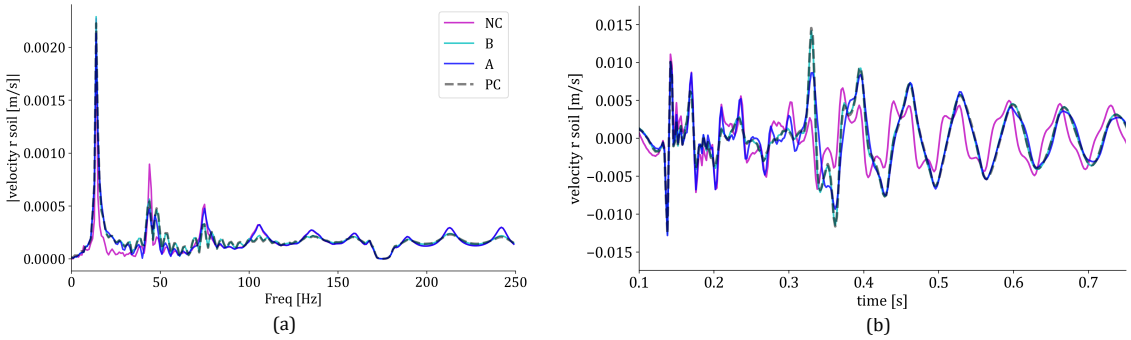

Figure 5: The soil velocities at the interface, r=40 m : (a) Frequency response of the radial velocity under 1MN constant-amplitude frequency sweep, and (b) Time-domain representation of the radial velocity.

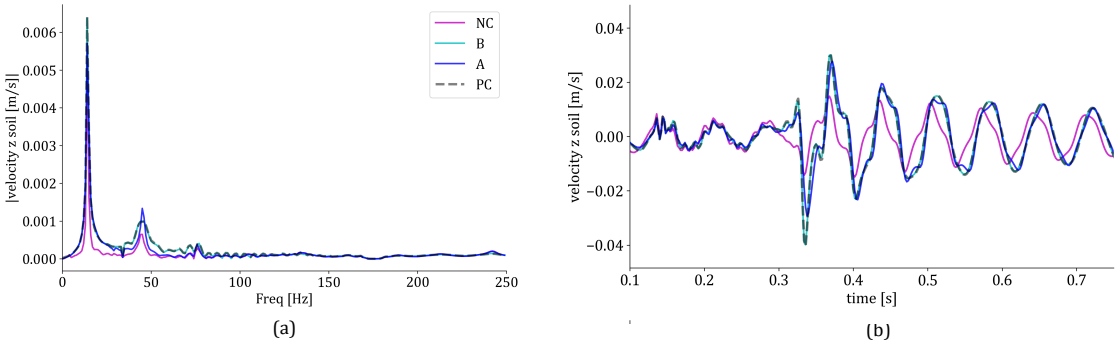

Figure 6: The soil velocities at the interface at r =40m and z=20m: (a) Frequency response of the vertical velocity under 1MN constant-amplitude frequency sweep, and (b) Time-domain representation of the vertical velocity

4. CONCLUSION AND FUTURE WORK

This study concludes that incorporating contact interface formulation enhances pile dynamics by relaxing the perfect contact constraint at the soil–pile interface. The results for impact pile driving are consistent with the vibro-pile prediction model proposed by [6], particularly in demonstrating a reduction in wave amplitudes at the soil–fluid interface. Furthermore, fluid pressure oscillations increase as the pile–soil interface becomes more relaxed. Given that fluid pressure and particle motion near the seabed can significantly affect marine life—especially benthic species such as invertebrates and bottom-dwelling fish—these findings underscore the importance of accurately modeling interface behavior.

Looking forward, future work will focus on improving the modeling approach by treating the contact mechanism parameter as a calibration variable for soil characterization, validated against experimental data. Another area of development will be to incorporate more advanced models for contact mechanism that reflect media-specific behavior, like Maxwell-type spring-dashpot models for mud-like seabed conditions. The model will also be expanded to include depth and frequency-dependent soil properties, accounting for variations in density, contact behavior, and compressional and shear wave velocities.

5. ACKNOWLEDGEMENT

The authors gratefully acknowledge SEASOUNDS for providing financial support for this research project. SEASOUNDS has received funding from the European Union's Horizon Programme under the Marie Skłodowska-Curie actions HORIZON-MSCA-2022-DN-01 (Grant agreement ID: 101119769

REFERENCES

[1] M. Solé, K. Kaifu, T. A. Mooney, S. L. Nedelec, F. Olivier, A. N. Radford, M. Vazzana, M. A. Wale, J. M. Semmens, S. D. Simpson, G. Buscaino, A. Hawkins, N. A. de Soto, T. Akamatsu, L. Chauvaud, R. D. Day, Q. Fitzgibbon, R. D. McCauley, M. André: "Marine invertebrates and noise", *Frontiers in Marine Science* **10**, (2023).

[2] A. D. Hawkins, R. A. Hazelwood, A. N. Popper, P. C. Macey: "Substrate vibrations and their potential effects upon fishes and invertebrates", *Journal of the Acoustical Society of America* **149**(4), 2782–2790 **(2021)**.

[3] A. Tsouvalas, A. V. Metrikine: "A three-dimensional vibroacoustic model for the prediction of underwater noise from offshore pile driving", *Journal of Sound and Vibration* **333**, 2283-2311 **(2014)**.

[4] Y. Peng, A. Tsouvalas, T. Stampoultzoglou, A. Metrikine: "A fast computational model for near- and far-field noise prediction due to offshore pile driving", *The Journal of the Acoustical Society of America* **149**(3), 1772–1790 **(2021)**.

[5] A. Tsetas, A. Tsouvalas, A. V. Metrikine: "A non-linear three-dimensional pile–soil model for vibratory pile installation in layered media", *International Journal of Solids and Structures* **269**, (2023).

[6] T. Molenkamp, A. Tsetas, A. Tsouvalas, A. Metrikine: "Underwater noise from vibratory pile driving with non-linear frictional pile–soil interaction", Journal of Sound and Vibration 576, (2024).

[7] T. Bohne, T. Grießmann, R. Rolfes: "Comprehensive analysis of the seismic wave fields generated by offshore pile driving: A case study at the BARD Offshore 1 offshore wind farm", *The Journal of the Acoustical Society of America* **155**, 1856-1867 **(2024)**.

[8] T. Di, W. Wu, Y. Zhang, Z. Wang, X. Liu, M. Xu, G. Mei: "Semi-analytical approach for nondestructive test for offshore pipe piles considering soil-pile slippage induced by heavy hammer impact", *Ocean Engineering* **260**, 112080 **(2022)**.